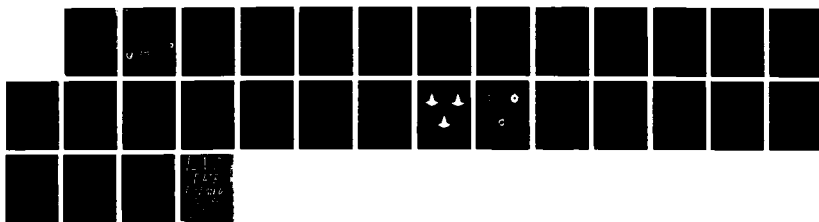


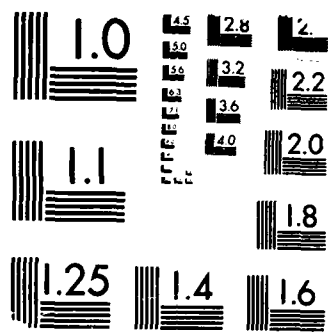
AD-A193 560 AN ADAPTIVE OVERLAPPING LOCAL GRID REFINEMENT METHOD
FOR TWO-DIMENSIONAL. (U) ARMY ARMAMENT RESEARCH
DEVELOPMENT AND ENGINEERING CENTER WAT.
UNCLASSIFIED P K MOORE ET AL. FEB 88 ARCCB-TR-88010

1/1

F/G 12/1

NL





MICROCOPY RESOLUTION TEST CHART
MIREAU - STANDARDS 1963 A

DTIC FILE COPY

(4)

AD

TECHNICAL REPORT ARCCB-TR-88010

AD-A193 560

**AN ADAPTIVE OVERLAPPING LOCAL
GRID REFINEMENT METHOD FOR
TWO-DIMENSIONAL PARABOLIC SYSTEMS**

PETER K. MOORE

JOSEPH E. FLAHERTY

FEBRUARY 1988

DTIC
SELECTED
APR 13 1988
S D
O N E



**US ARMY ARMAMENT RESEARCH,
DEVELOPMENT AND ENGINEERING CENTER
CLOSE COMBAT ARMAMENTS CENTER
BENÉT LABORATORIES
WATERVLIET, N.Y. 12189-4050**



APPROVED FOR PUBLIC RELEASE; DISTRIBUTION UNLIMITED

88 4 12 065

DISCLAIMER

The findings in this report are not to be construed as an official Department of the Army position unless so designated by other authorized documents.

The use of trade name(s) and/or manufacturer(s) does not constitute an official indorsement or approval.

DESTRUCTION NOTICE

For classified documents, follow the procedures in DoD 5200.22-M, Industrial Security Manual, Section II-19 or DoD 5200.1-R, Information Security Program Regulation, Chapter IX.

For unclassified, limited documents, destroy by any method that will prevent disclosure of contents or reconstruction of the document.

For unclassified, unlimited documents, destroy when the report is no longer needed. Do not return it to the originator.

SECURITY CLASSIFICATION OF THIS PAGE (When Data Entered)

REPORT DOCUMENTATION PAGE		READ INSTRUCTIONS BEFORE COMPLETING FORM
1. REPORT NUMBER ARCCB-TR-88010	2. GOVT ACCESSION NO.	3. RECIPIENT'S CATALOG NUMBER
4. TITLE (and Subtitle) AN ADAPTIVE OVERLAPPING LOCAL GRID REFINEMENT METHOD FOR TWO-DIMENSIONAL PARABOLIC SYSTEMS		5. TYPE OF REPORT & PERIOD COVERED Final
7. AUTHOR(s) Peter K. Moore and Joseph E. Flaherty (See reverse)		6. PERFORMING ORG. REPORT NUMBER
9. PERFORMING ORGANIZATION NAME AND ADDRESS US Army ARDEC Benet Laboratories, SMCAR-CCB-TL Watervliet, NY 12189-4050		10. PROGRAM ELEMENT, PROJECT, TASK AREA & WORK UNIT NUMBERS AMCMS No. 6126.23.1BL0.0 PRON No. 1A72ZJ5MNMSC
11. CONTROLLING OFFICE NAME AND ADDRESS US Army ARDEC Close Combat Armaments Center Picatinny Arsenal, NJ 07806-5000		12. REPORT DATE February 1988
14. MONITORING AGENCY NAME & ADDRESS(if different from Controlling Office)		13. NUMBER OF PAGES 22
		15. SECURITY CLASS. (of this report) UNCLASSIFIED
		15a. DECLASSIFICATION/DOWNGRADING SCHEDULE
16. DISTRIBUTION STATEMENT (of this Report) Approved for public release; distribution unlimited.		
17. DISTRIBUTION STATEMENT (of the abstract entered in Block 20, if different from Report)		
18. SUPPLEMENTARY NOTES Presented at the Fifth Army Conference on Applied Mathematics and Computing, U.S. Military Academy, West Point, New York, 15-18 June 1987. Published in Proceedings of the Conference.		
19. KEY WORDS (Continue on reverse side if necessary and identify by block number) → Finite Element Methods Adaptive Methods Overlapping Grids Local Refinement Parabolic Systems		
20. ABSTRACT (Continue on reverse side if necessary and identify by block number) We present an adaptive local refinement finite element method for solving vector systems of parabolic partial differential equations in two-space dimensions and time. The algorithm uses the finite element-Galerkin method in space and backward Euler temporal integration. At each time step we obtain an estimate of the error on each element, group the elements whose error violates a user prescribed tolerance, form new local grids, and solve the (CONT'D ON REVERSE)		

7. AUTHORS (CONT'D)

Peter K. Moore
Department of Computer Science
Rensselaer Polytechnic Institute
Troy, NY 12180-3590

Joseph E. Flaherty
Department of Computer Science
Rensselaer Polytechnic Institute
Troy, NY 12180-3590

and

US Army ARDEC
Close Combat Armaments Center
Benet Laboratories
Watervliet, NY 12189-4050

20. ABSTRACT (CONT'D)

problem again on each of the new grids. We discuss several aspects of the algorithm including the necessary data structures, the error estimation technique, and the determination of initial and boundary conditions at coarse-fine mesh interfaces. Finally, we present several examples which demonstrate the viability of our approach. *Keywords:* ...

Classification	
UNCLASSIFIED	
Distribution	
Availability Codes	
1	2
3	4
A-1	



UNCLASSIFIED

TABLE OF CONTENTS

	<u>Page</u>
I. INTRODUCTION	1
II. LOCAL REFINEMENT AND DATA STRUCTURES	4
III. SPATIAL AND TEMPORAL DISCRETIZATION	8
IV. EXAMPLES	12
Example 1	12
Example 2	13
Example 3	14
V. CONCLUSIONS	17
REFERENCES	19

TABLES

1. Error and effectivity ratio for one time step and uniform spatial meshes of spacing π/J for Example 1. 13
2. Error and effectivity ratio for one time step and uniform spatial meshes of spacing π/J for Example 2. 14
3. Maximum difference between solutions on the boundaries of overlapping grids after each Schwarz iteration. 17

LIST OF ILLUSTRATIONS

1. Coarse spatial background mesh with two offspring megagrids (marked with diamonds and squares) and their local grids. High-error elements of the coarse mesh are indicated by x's. 3
2. Recursive local refinement algorithm for the solution of Eq. (1) on $R(w,p,q,F,S,L)$ with an error tolerance tol. 5
3. Solution algorithm on megagrid $R(w,p,q,F,S,L)$. 6
4. Surface renditions of the solution of Example 2 at $t = 0.3$, 0.5, and 0.8. 15
5. Contour plots of the solution of Example 2 at $t = 0.3$, 0.5, and 0.8. 16
6. Local grids introduced after the initial time step for Example 3. The original coarse grid is also shown. 18

I. INTRODUCTION.

Over the past several years extensive efforts have been made in using adaptive strategies to solve partial differential equations [2, 3]*. In this report, we consider a local mesh refinement procedure for two-dimensional parabolic partial differential systems where fine meshes are introduced in regions where greater resolution is deemed necessary. Our approach permits finer meshes to overlap elements of coarser ones and is related to an earlier effort on h-refinement methods for one-dimensional parabolic problems [5, 7, 10].

We consider an initial-boundary value problem for an m -dimensional vector system having the form

$$\mathbf{u}_t + \mathbf{f}(x, y, t, \mathbf{u}, \mathbf{u}_x, \mathbf{u}_y) = [\mathbf{D}_1(x, y, t, \mathbf{u})\mathbf{u}_x]_x + [\mathbf{D}_2(x, y, t, \mathbf{u})\mathbf{u}_y]_y, \quad (x, y) \in \Omega, \quad t > 0, \quad (1a)$$

$$\mathbf{u}(x, y, 0) = \mathbf{u}_0(x, y), \quad (x, y) \in \Omega \cup \partial\Omega, \quad (1b)$$

$$\mathbf{u}(x, y, t) = \mathbf{g}_D(x, y, t), \quad (x, y) \in \partial\Omega_D, \quad t > 0, \quad (1c)$$

$$\mathbf{D}_1\mathbf{u}_x\eta^1 + \mathbf{D}_2\mathbf{u}_y\eta^2 = \mathbf{g}_N(x, y, t), \quad (x, y) \in \partial\Omega_N, \quad t > 0. \quad (1d)$$

The domain Ω is the rectangle $\{(x, y) \mid a < x < b, c < y < d\}$ with boundary $\partial\Omega = \partial\Omega_D \cup \partial\Omega_N$ and unit outer normal $\boldsymbol{\eta} := [\eta^1, \eta^2]^T$. The system in Eq. (1) is assumed to be well posed and parabolic, i.e., \mathbf{D}_1 and \mathbf{D}_2 are positive definite. We do not expect that our methods will be able to solve all problems having this generality, but our one-dimensional procedure [10] has worked well on a wide range of linear and nonlinear problems.

* References are listed at the end of this report.

Our approach begins with the solution of Eq. (1) on a uniform space-time grid using finite elements in space and the backward Euler method in time. At the end of each time step, an indication of the local discretization error is generated on each finite element. In our initial investigation of one-dimensional problems [5, 7], we used an h-refinement (Richardson's extrapolation) procedure to compute a local error indicator. This has subsequently been abandoned in favor of a p-refinement approach [10], which increases the order of the trial space instead of reducing the mesh spacing. The p-refinement strategy employs nodal superconvergence to improve computational efficiency and it can be used to generate an asymptotically correct estimate of the discretization error [1, 10]. Elements having high error are grouped into rectangular regions called *megagrids* using a nearest neighbor clustering algorithm (cf. Berger and Oliger [4]). Overlapping fine uniform grids are generated within the megagrids and Eq. (1) is solved again on these grids. This process is repeated until a prescribed local error tolerance is satisfied. An illustration of a coarse spatial mesh with two megagrids and three fine grids is shown in Figure 1.

A tree is a natural data structure to manage the information associated with all of the grids. Nodes of the tree represent data at the megagrid level, with finer megagrids regarded as offspring of coarser ones. Information associated with overlapping fine grids within each megagrid is stored as records at the nodes of the tree.

A finite element problem is formulated and solved on each grid within a megagrid. This necessitates the prescription of appropriate initial and boundary conditions on each space-time grid. Since our temporal integration is implicit, prescribing boundary conditions is particularly complex in regions where meshes overlap (Figure 1). An iterative procedure, analogous to Schwarz alternation (cf. Dihl et al. [6]), is used to successively calculate solutions on fine grids within each megagrid. We

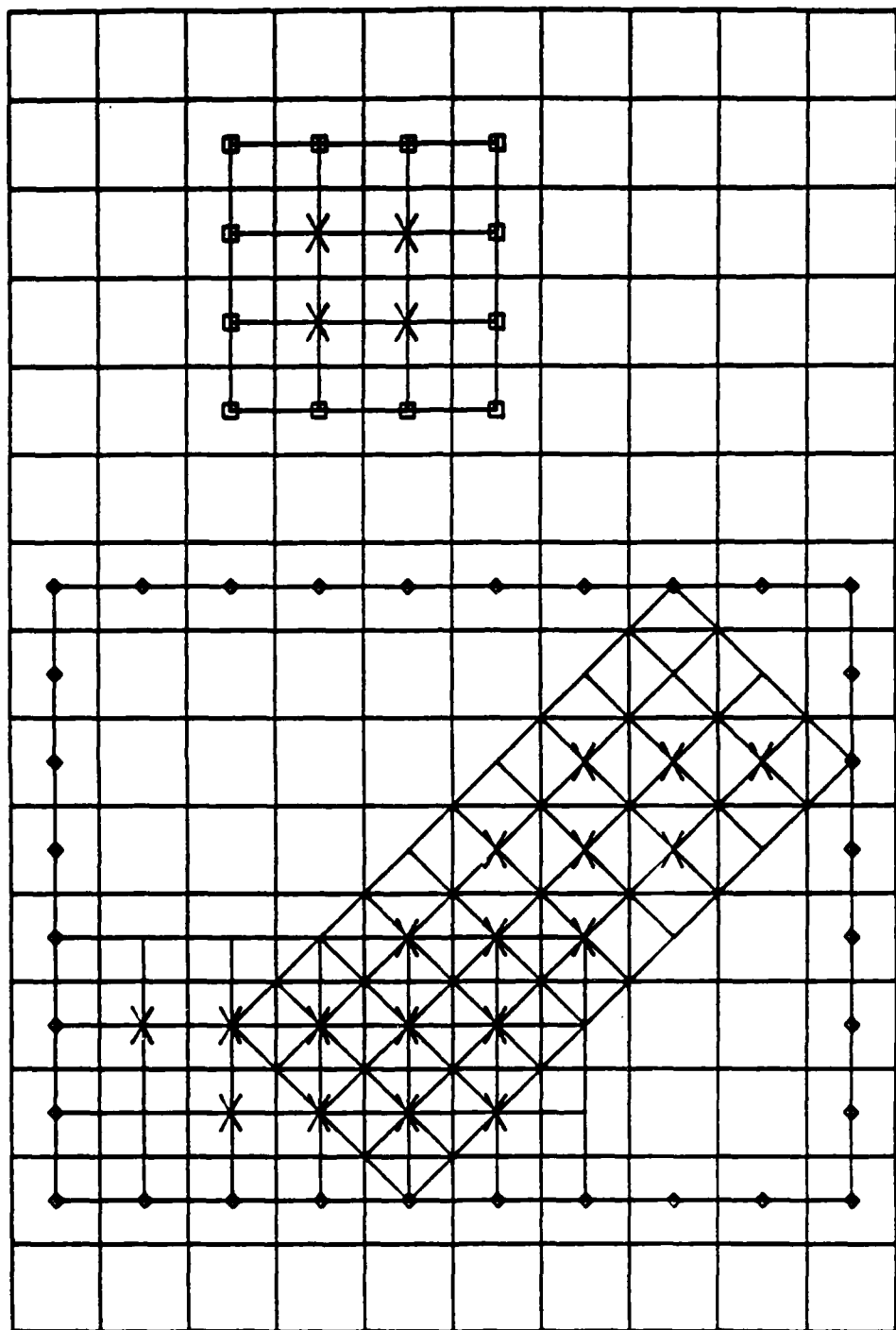


Figure 1. Coarse spatial background mesh with two offspring megagrids (marked with diamonds and squares) and their local grids. High-error elements of the coarse mesh are indicated by X's.

observe that this procedure converges for a variety of problems, but have no analysis demonstrating either convergence or stability. Starius [11] obtained some stability results on a similar method for hyperbolic equations.

A description of the data structures and the local refinement procedure is given in Section II. In Section III we present the finite element method and the local error estimation technique. Section IV contains some preliminary computation results on three linear parabolic problems. Our conclusions and plans for further improvements are described in Section V. The examples indicate that the error estimation procedure converges to the true discretization error as the mesh is refined, and the solution procedure based on the Schwarz alternating technique converges.

II. LOCAL REFINEMENT AND DATA STRUCTURES.

We outline our procedure for solving Eq. (1) on an arbitrary hexahedral megagrid $R(\omega, p, q, F, S, L)$. The domain $\omega := \{(x, y) \mid \alpha < x < \beta, \gamma < y < \delta\}$; p and q are the times at the beginning and end of the time step, respectively; F and S point to the parent and offspring megagrids, respectively; and L is the record of information for the σ local rectangular grids within R .

A top level description of our local refinement algorithm is presented in Figure 2. Solution and error indicators are generated on R using procedure `solve` (Figure 3). Elements where the error indicator exceeds a prescribed tolerance tol are partitioned into rectangular regions using the nearest neighbor clustering algorithm. As noted, we call these regions megagrids. Berger and Oliger's [4] bisection and merging procedure is used to generate local uniform fine grids for each megagrid. Local grids within a megagrid can overlap, but the megagrids are independent of each other; hence, each offspring megagrid may have different spatial and temporal refinement factors. This

also reduces communication between megagrids, and thus, simplifies the computation of initial conditions on offspring megagrids. This representation may additionally be suitable for execution on parallel computers. Temporal refinement factors are calculated and solutions are recursively generated for each megagrid.

```

procedure locref ( $R(\omega, p, q, F, S, L)$ , tol);
begin
  solve ( $R(\omega, p, q, F, S, L)$ );
  if any error indicator > tol then
    begin
      Form offspring megagrids;
      for  $j := 1$  to number of offspring do
        Create local rectangular grids;
        for  $j := 1$  to number of offspring do
          Calculate the temporal refinement factor  $tref[j]$ ;
          for  $j := 1$  to number of offspring do
            for  $i := 1$  to  $tref[j]$  do
              begin
                 $p[i] := p + (i-1)*(q-p)/tref[j];$ 
                 $q[i] := p[i] + (q-p)/tref[j];$ 
                locref ( $R(\omega[j], p[i], q[i],$ 
 $R(\omega, p, q, F, S, L), S[j], L[j])$ , tol)
              end
            end
          end { locref };

```

Figure 2. Recursive local refinement algorithm for the solution of Eq. (1) on $R(\omega, p, q, F, S, L)$ with an error tolerance tol .

In order to solve the problem in Eq. (1), the procedure locref is invoked on the coarse grids $R(\Omega, t_k, t_{k+1}, 0, S, L)$, $k = 0, 1, \dots$. Solutions satisfying the prescribed accuracy requirements are generated at each time t_k , $k = 1, 2, \dots$.

The solution on a megagrid $R(\omega, p, q, F, S, L)$ is described by the procedure solve of Figure 3. Initial conditions are generated for each local computation grid contained in R . Following this, we compute an initial guess for the boundary conditions of the

local grids using either the prescribed boundary data at physical boundaries or linear interpolation in time from the parent megagrid of R . A finite element solution is generated for one of the local grids and its solution is used to update boundary conditions on all other intersecting local grids. This solution process is repeated on each local grid in turn until satisfactory convergence is attained. Our procedure is, thus, similar to the Schwarz alternating principle for elliptic problems, which has been used recently to develop domain decomposition methods for parallel computation [6, 8].

```

procedure solve ( $R(\omega, p, q, F, S, L)$ );
begin
  for  $i := 1$  to number of local grids do
    begin
      Compute initial conditions for local grid
       $T((x_m)_i, (y_m)_i, (d_x)_i, (d_y)_i, s_i);$ 
      Compute boundary conditions for
       $T((x_m)_i, (y_m)_i, (d_x)_i, (d_y)_i, s_i);$ 
    end
  for  $j := 1$  to number of iterations do
    for  $i := 1$  to number of local grids do
      begin
        Solve the finite element problem for Eq. (1) on
         $T((x_m)_i, (y_m)_i, (d_x)_i, (d_y)_i, s_i);$ 
        if  $j =$  number of iterations then
          Compute error on  $T((x_m)_i, (y_m)_i, (d_x)_i, (d_y)_i, s_i)$ 
          Update appropriate boundary conditions
      end
    end { solve } ;

```

Figure 3. Solution algorithm on megagrid $R(\omega, p, q, F, S, L)$.

A local grid is denoted as $T(x_m, y_m, d_x, d_y, s)$. Each local rectangular grid is characterized by the coordinates of its center (x_m, y_m) , the lengths of its sides d_x and d_y , and the slope s of a side of the rectangle. In order to avoid ambiguity, we choose $s \geq 0$ and let d_x correspond to this side (Figure 1). The number of elements $m_i \times n_i$

on local grid $T_i = T((x_m)_i, (y_m)_i, (d_x)_i, (d_y)_i, s_i)$ is determined by a single mesh spacing parameter h_R as $m_i = \text{round}(d_x/h_R)$ and $n_i = \text{round}(d_y/h_R)$. Thus, each local grid in R has approximately the same spatial resolution. Many details of this algorithm have been omitted and additional information is presented in Moore [9]. For example, a strategy has been developed for storing the finite element solution at p and q without unnecessary duplication or copying of information.

Initial conditions for each local grid are either determined from Eq. (1b) when $p = 0$ or by bilinear interpolation using the finest grids available in the tree structure at time $p > 0$. Isolating local grids within megagrids greatly simplifies the search for data needed for this bilinear interpolation. Thus, the search for a solution value at an arbitrary point is performed at the megagrid level until the finest megagrid containing the point has been identified. The local grids of this finest megagrid provide the necessary interpolation data. Scanning the points of a grid in a predetermined order can be used to further reduce the complexity of the search procedure.

Similar considerations are required to determine boundary conditions on grid edges that are not subsets of $\partial\Omega$. Our one-dimensional techniques [10] and the explicit finite difference procedures of Berger and Oliger [4] used the notion of a "buffer" to apply boundary conditions. The idea is to enlarge a local rectangular grid by increasing d_x and d_y by two or four elements so that "artificial boundary conditions" may be obtained from data in low-error regions. However, in regions where local grids overlap, accurate boundary conditions cannot be obtained from parent grid data even with a buffer. Buffers do provide accurate boundary conditions in regions where grids do not overlap and, for this reason, we continue to use them.

Dirichlet boundary conditions are obtained on the edges of buffered local grids by piecewise bilinear interpolation in time using solution values from the parent megagrid. In non-overlapping buffered regions, the interpolated boundary conditions satisfy the prescribed error tolerance, and are thus expected to produce acceptable accuracy. As noted, accurate boundary conditions are obtained in regions where local grids overlap by means of the Schwarz alternating principle. Hence, we initially solve a finite element problem on local grid T_1 of R , realizing that the interpolated boundary data may be inaccurate in regions where T_1 intersects other local grids. In solving the problem on T_2 we use boundary data from T_1 with bilinear interpolation in regions where T_1 and T_2 intersect. This sequential updating procedure can be continued iteratively until satisfactory convergence is obtained. In practice, we halt the iteration after a few cycles and compute an error estimate for each local grid in R . The grids of R are refined if the error tolerance is not satisfied. Thus, we do not distinguish between failure of the Schwarz iteration to converge and failure to satisfy prescribed accuracy conditions.

Treatment of situations where local grids overlap $\partial\Omega$ are considerably more complex. A second complication arises when a local grid crosses the boundary of $\sigma_F \cup (T_F)_i$, where the subscript F denotes the parent megagrid of R . These issues are handled by regridding as described in Moore [9].

III. SPATIAL AND TEMPORAL DISCRETIZATION.

As noted, the partial differential system in Eq. (1) is discretized on a local grid T of R using a finite element Galerkin procedure in space and the backward Euler method in time. For each time $t \in [p, q]$, we assume that $u \in H_E^1$ and select a test

function $\mathbf{v} \in H_0^1$, where H^1 denotes the usual Sobolev space. Functions that further satisfy Dirichlet conditions on ∂T are said to belong to H_E^1 , while functions satisfying trivial Dirichlet conditions belong to H_0^1 .

The Galerkin form of Eq. (1) on T is

$$(\mathbf{v}, \mathbf{u}_t) + (\mathbf{v}, \mathbf{f}(\cdot, \cdot, t, \mathbf{u}, \mathbf{u}_x, \mathbf{u}_y)) + A(\mathbf{v}, \mathbf{u}) = \int_{\partial T \cap \partial \Omega_N} \mathbf{v}^T \mathbf{g}_N ds, \quad \text{for all } \mathbf{v} \in H_0^1, \quad (2a)$$

where

$$(\mathbf{v}, \mathbf{u}) = \int_T \mathbf{v}^T \mathbf{u} dx dy, \quad (2b)$$

$$A(\mathbf{v}, \mathbf{u}) = \int_T [\mathbf{v}_x^T \mathbf{D}_1(x, y, t, \mathbf{u}) \mathbf{u}_x + \mathbf{v}_y^T \mathbf{D}_2(x, y, t, \mathbf{u}) \mathbf{u}_y] dx dy. \quad (2c)$$

Initial conditions are required at $p = 0$ and these can be obtained, e.g., by L^2 or H^1 projection. Initial conditions for $p > 0$ trivially follow from the solution at the end of the previous time step.

A finite element solution of Eq. (2) is obtained by approximating H^1 by a finite dimensional subspace K of piecewise bilinear polynomials on T . The finite element solution \mathbf{U} satisfies

$$(\mathbf{V}, \mathbf{U}_t) + (\mathbf{V}, \mathbf{f}(\cdot, \cdot, t, \mathbf{U}, \mathbf{U}_x, \mathbf{U}_y)) + A(\mathbf{V}, \mathbf{U}) = \int_{\partial T \cap \partial \Omega_N} \mathbf{V}^T \mathbf{g}_N ds, \\ \text{for all } \mathbf{V} \in K_0. \quad (3a)$$

$$\mathbf{U}(x, y, p) = \begin{cases} \mathbf{P}(\mathbf{u}_0), & p = 0 \\ \mathbf{P}(\mathbf{U}(\cdot, \cdot, p^-)), & p > 0. \end{cases} \quad (3b)$$

The projection \mathbf{P} at $p = 0$ is obtained by constructing a piecewise bilinear approximation of \mathbf{u}_0 . For $p > 0$, we proceed in a similar manner except that we construct interpolants using the finest grid solution available at $t = p^-$.

Temporal discretization of Eq. (3) is performed by the backward Euler method; thus, we determine $\mathbf{U}^q(x,y)$ as discrete approximation of $\mathbf{U}(x,y,q)$ by solving

$$\begin{aligned} (\mathbf{V}, \mathbf{U}^q) + \Delta t [(\mathbf{V}, \mathbf{f}(\cdot, \cdot, t, \mathbf{U}^q, \mathbf{U}_x^q, \mathbf{U}_y^q)) + A(\mathbf{V}, \mathbf{U}^q)] &= (\mathbf{V}, \mathbf{U}^p) + \\ \Delta t \int_{\partial T \cap \partial \Omega_N} \mathbf{V}^T \mathbf{g}_N(x, y, q) ds, \quad \text{for all } \mathbf{V} \in K_0, \end{aligned} \quad (4)$$

Initial conditions for the discrete system in Eq. (4) follow the lines of Eq. (3b) for the semi-discrete system.

A posteriori estimates of the discretization error of the solution of Eq. (4) are obtained by means of a p-refinement technique. To begin, we calculate a second solution $\mathbf{U}_Q^q(x,y)$ of Eq. (2) using piecewise quadratic polynomials in space and trapezoidal rule integration in time. This solution is higher order in both space and time than the solution of Eq. (4); thus, the difference $\|\mathbf{U}^q - \mathbf{U}_Q^q\|_1$ furnishes an estimate of the discretization error of \mathbf{U}^q . The computational efficiency of this procedure can be substantially improved by using the nodal superconvergence property of finite element methods for parabolic problems [1, 10]. Nodal superconvergence implies that bilinear finite element solutions converge at a faster rate in space at nodes than elsewhere. These considerations imply that \mathbf{U}_Q^q can be calculated as

$$\mathbf{U}_Q^q(x,y) \approx \hat{\mathbf{U}}_Q^q(x,y) = \hat{\mathbf{U}}^q(x,y) + \mathbf{E}^q(x,y), \quad (5)$$

where $\hat{\mathbf{U}}^q(x,y)$ is a piecewise bilinear function and $\mathbf{E}^q(x,y)$ is a piecewise serendipity function (a biquadratic polynomial less a quartic term) that vanishes at the nodes of T . Specifically, we find that $\hat{\mathbf{U}}^q(x,y)$ satisfies

$$(\mathbf{V}, \frac{\hat{\mathbf{U}}^q - \mathbf{U}^p}{\Delta t}) + \tfrac{1}{2} [(\mathbf{V}, \mathbf{f}(\cdot, \cdot, q, \hat{\mathbf{U}}^q, \hat{\mathbf{U}}_x^q, \hat{\mathbf{U}}_y^q)) + (\mathbf{V}, \mathbf{f}(\cdot, \cdot, p, \mathbf{U}^p, \mathbf{U}_x^p, \mathbf{U}_y^p))] +$$

$$\begin{aligned} \frac{1}{2}[A(\mathbf{V}, \hat{\mathbf{U}}^q) + A(\mathbf{V}, \mathbf{U}^p)] &= \frac{1}{2} \int_{\partial T \cap \partial \Omega_N} \mathbf{V}^T \mathbf{g}_N(x, y, q) ds + \frac{1}{2} \int_{\partial T \cap \partial \Omega_N} \mathbf{V}^T \mathbf{g}_N(x, y, p) ds \\ &\quad \text{for all } \mathbf{V} \in K_0. \end{aligned} \quad (6)$$

Thus, a trapezoidal rule integration step is performed using the backward Euler solution $\mathbf{U}^p(x, y)$ as an initial condition. Both Eqs. (4) and (6) are a nonlinear algebraic system which we solve by Newton's method. In order to reduce the computational effort associated with assembling and solving Eq. (6), the Jacobian of Eq. (4) is used for both Newton iterations. The solution of Eq. (4) is obtained first and the result $\mathbf{U}^q(x, y)$ is used as an initial guess for $\hat{\mathbf{U}}^q(x, y)$.

The piecewise quadratic correction $\mathbf{E}^q(x, y)$ satisfies

$$\begin{aligned} &(\mathbf{V}, [(\hat{\mathbf{U}}^q + \mathbf{E}^q) - (\mathbf{U}^p + \mathbf{E}^p)] / \Delta t) + \frac{1}{2}[(\mathbf{V}, \mathbf{f}(\cdot, \cdot, q, \hat{\mathbf{U}}^q + \mathbf{E}^q, \hat{\mathbf{U}}_x^q + \mathbf{E}_x^q, \hat{\mathbf{U}}_y^q + \mathbf{E}_y^q)) \\ &+ (\mathbf{V}, \mathbf{f}(\cdot, \cdot, p, \mathbf{U}^p + \mathbf{E}^p, \mathbf{U}_x^p + \mathbf{E}_x^p, \mathbf{U}_y^p + \mathbf{E}_y^p))] + \frac{1}{2}[A(\mathbf{V}, \hat{\mathbf{U}}^q + \mathbf{E}^q) + A(\mathbf{V}, \mathbf{U}^p + \mathbf{E}^p)] \\ &= \frac{1}{2} \int_{\partial T \cap \partial \Omega_N} \mathbf{V}^T \mathbf{g}_N(x, y, q) ds + \frac{1}{2} \int_{\partial T \cap \partial \Omega_N} \mathbf{V}^T \mathbf{g}_N(x, y, p) ds \text{ for all } \mathbf{V} \in K_0^Q. \end{aligned} \quad (7)$$

As noted, the space K_0^Q consists of piecewise serendipity functions that vanish at the vertices of the elements. Trivial initial conditions are used in the solution of Eq. (7) for $p > 0$. Interpolated values of the initial error $\mathbf{u}^0(x, y) - \mathbf{U}(x, y, 0)$ onto K_0^Q are used at $p = 0$.

Linear systems associated with the application of Newton's iteration to Eqs. (4), (6), and (7) are solved by the Lanczos acceleration of the Jacobi iterative method as implemented in the iterative solution package ITPACK of Young and Mai [12].

IV. EXAMPLES.

We consider a sequence of three linear problems that are designed to illustrate the performance of our error estimation and local refinement procedures and convergence of the Schwarz iteration. Our results are very preliminary, and additional computational work and analysis will be necessary before firm conclusions can be drawn.

Performance of our error estimation technique is measured by the effectivity ratio

$$\theta = \frac{\|U^q - \hat{U}_Q^q\|_1}{\|u(x,y,q) - U^q\|_1}, \quad (8)$$

which is a ratio of the estimated to the actual error in the H_1 norm. Ideally, the effectivity ratio should approach unity as the mesh is refined and should not differ substantially from unity over a large range of mesh spacings. The convergence of our error estimate to the true discretization error has been established for one-dimensional linear problems [10].

Example 1. Consider the linear constant coefficient heat conduction problem on $\Omega := \{(x,y) \mid 0 < x, y < \pi\}$

$$u_t = \frac{1}{2}(u_{xx} + u_{yy}), \quad (x,y) \in \Omega, \quad t > 0, \quad (9a)$$

$$u(x,y,0) = \sin x \sin y, \quad (x,y) \in \Omega \cup \partial\Omega, \quad (9b)$$

$$u(x,y,t) = 0, \quad (x,y) \in \partial\Omega, \quad t > 0. \quad (9c)$$

The exact solution of this problem is

$$u(x,y,t) = e^{-t} u(x,y,0). \quad (10)$$

We solved Eq. (9) for a single time step on uniform grids having equal temporal

and spatial mesh spacings of π/J , $J = 10, 20, 40$. The exact error and effectivity ratio are presented in Table 1. The results indicate that the finite element solution is converging at a linear rate and that the effectivity ratio is converging to unity.

J	$\ u(x,y,\Delta t) - U^\Delta\ _1$	θ
10	0.1578	1.050
20	0.0882	1.012
40	0.0469	1.003

Table 1. Error and effectivity ratio for one time step and uniform spatial meshes of spacing π/J for Example 1.

Example 2. Consider the forced heat conduction equation on $\Omega := \{(x,y) | 0 < x, y < 1\}$

$$u_t + f(x,y,t) = u_{xx} + u_{yy}, \quad (x,y) \in \Omega, \quad t > t_0, \quad (11)$$

with $f(x,y,t)$ and the initial and Dirichlet boundary conditions specified so that the exact solution is

$$u(x,y,t) = \sin \pi t e^{t-20[(x-1/2)^2+(y-1/2)^2]}. \quad (12)$$

With $t_0 = 0.5$, we solve Eq. (11) for one time step on uniform grids having equal temporal and spatial meshes of $1/J$, $J = 10, 20, 40$. Results similar to those of Example 1 are displayed in Table 2. Thus, once again, the error is converging to zero at a linear rate and the effectivity ratio is tending to unity and is close to unity for all meshes. In this example, as opposed to Example 1, the effectivity ratio appears to be converging to unity from below. In practice, an upper bound is more suited to an adaptive local refinement procedure.

J	$\ u(x,y,\Delta t) - U^{\Delta t}\ _1$	θ
10	0.6796	0.996
20	0.3383	0.998
40	0.1668	0.999

Table 2. Error and effectivity ratio for one time step and uniform spatial meshes of spacing π/J for Example 2.

We also solve Eq. (11) for $0 = t_0 \leq t \leq 1$ using the adaptive local refinement strategy of Section II with a tolerance of 0.05 and an initial 10×10 mesh having a time step of 0.1. Surface renditions and contour plots of the solution at $t = 0.3, 0.5,$ and 0.8 are shown in Figures 4 and 5, respectively.

Example 3. Consider the forced heat conduction equation (11) on $\Omega := \{(x,y) | 0 < x, y < 1\}$ with $f(x,y,t)$ and the initial and Dirichlet boundary conditions specified so that the exact solution is

$$u(x,y,t) = 1.0 - \tanh[10(x+y-t-0.45)]. \quad (13)$$

This example is used to verify convergence of the Schwarz alternating principle. The problem is solved for a single time step with $t_0 = 0.5$ on an initial uniform coarse 10×10 mesh having a time step of 0.1 and a tolerance of 0.05. Refinement was needed at the initial time and 10 local grids, as shown in Figure 6, were introduced. The initial coarse mesh is also shown as a reference. Schwarz iterations were performed on these grids and we measure the difference in successive solutions on alternating grids on the portions of the boundaries of each local grid in regions where they overlap. The maximum such difference after each Schwarz iteration is shown in Table

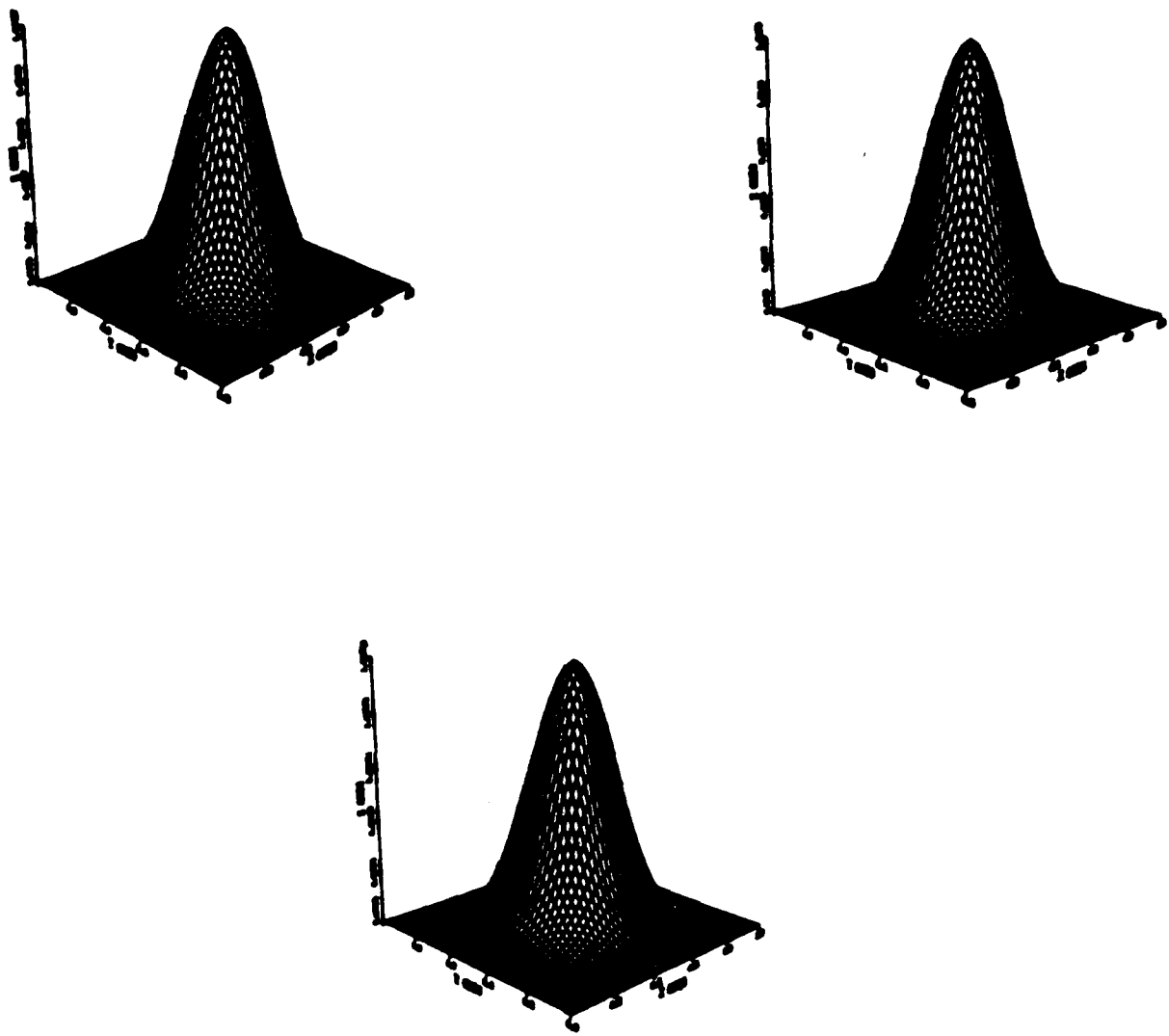


Figure 4. Surface renditions of the solution of Example 2 at $t = 0.3$ (upper left), 0.5 (upper right), and 0.8 (lower center).

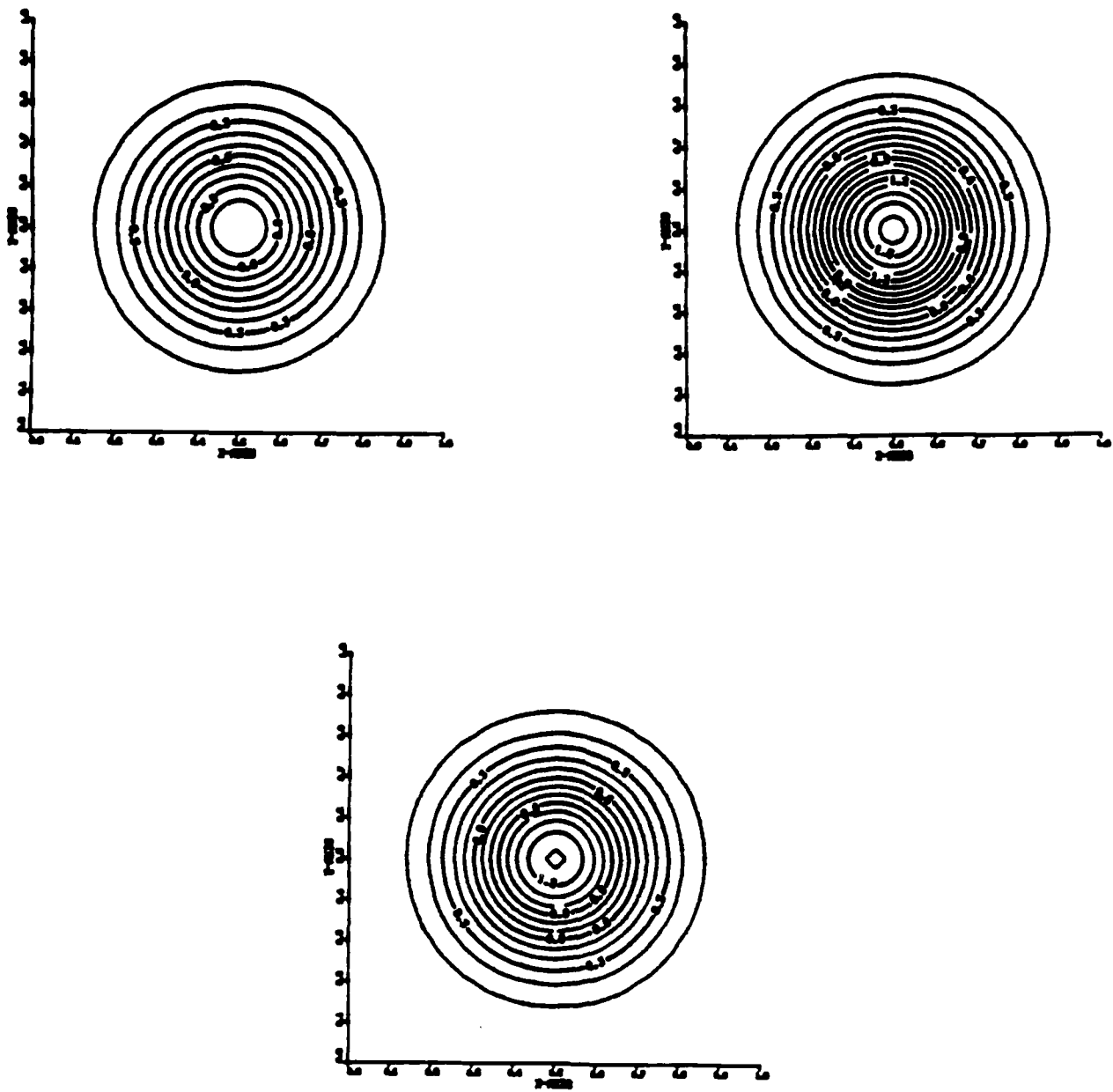


Figure 5. Contour plots of the solution of Example 2 at $t = 0.3$ (upper left), 0.5 (upper right), and 0.8 (lower center).

3. It appears that the iteration is converging at nearly a quadratic rate.

Iteration	Maximum Difference
1	0.1506
2	0.0114
3	0.0016
4	0.0004

Table 3. Maximum difference between solutions on the boundaries of overlapping grids after each Schwarz iteration.

V. CONCLUSIONS.

We developed an adaptive local mesh refinement procedure for nonlinear parabolic systems on rectangular regions. A complex tree data structure is used to manage a nest of local overlapping grids. An implicit finite element solution strategy using piecewise linear approximations and the backward Euler method is formulated. We obtain an estimate of the local discretization error of these finite element solutions using a p-hierarchical approach with piecewise serendipity approximations and trapezoidal rule integration. The Schwarz alternating principle is used to calculate boundary conditions on portions of local grids that overlap.

Our results indicate that the error estimation procedure converges to the exact local error as the mesh is refined. As noted, a proof of this convergence has been established for certain linear one-dimensional problems (cf. Moore and Flaherty [10]). It should be possible to construct a proof of convergence of the two-dimensional error estimate using the ideas developed in the one-dimensional case. The use of the

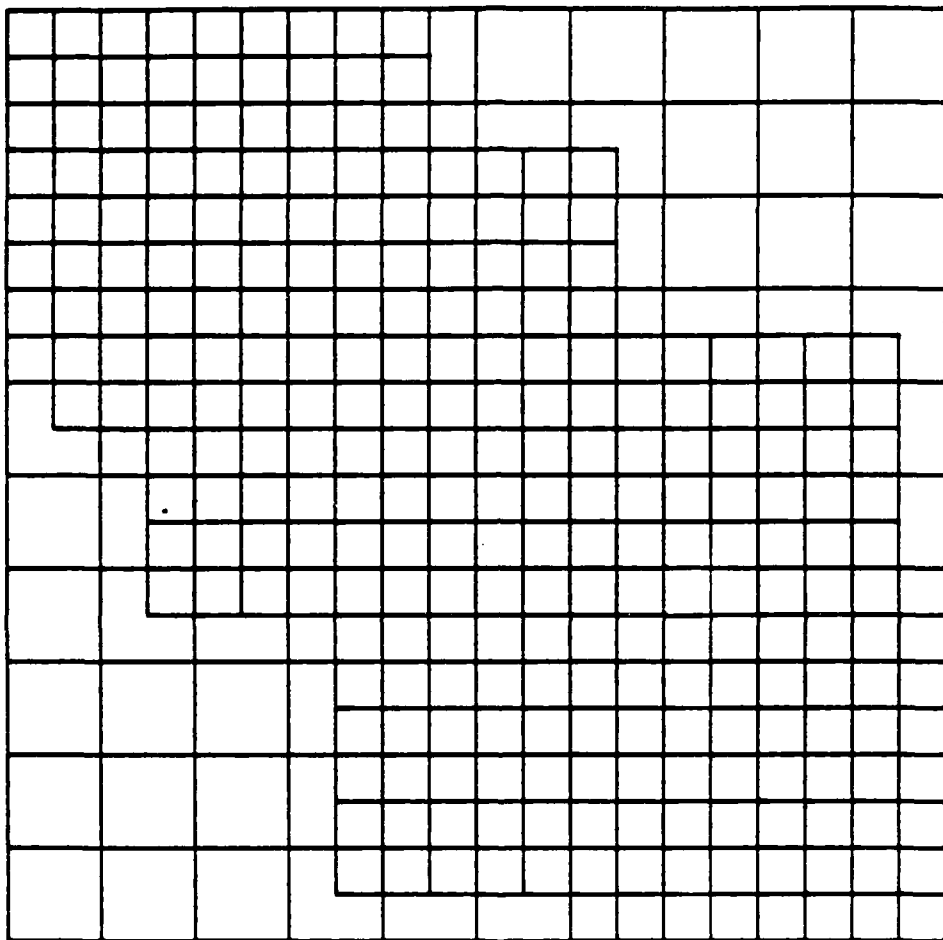


Figure 6. Local grids introduced after the initial time step for Example 3.
The original coarse grid is also shown.

Schwarz alternating principle also appears to be a very efficient method of calculating boundary conditions in overlapping-grid regions.

We are encouraged by the performance of our methods on these preliminary problems; however, several aspects of our approach need improvement. The Lanczos iteration used to solve the linear system appeared to be far less than optimal. The stopping criteria used in the ITPACK [12] implementation was too conservative for our applications. Creation of local solution grids is difficult and complex near domain boundaries. At present we know of no way of improving this defect. We have plans of extending our methods to non-rectangular domains using an overlapping-grid mesh generation procedure.

REFERENCES

1. S. Adjerid and J.E. Flaherty, "Local Refinement Finite Element Methods on Stationary and Moving Meshes for One-Dimensional Parabolic Systems," 1987, in preparation.
2. I. Babuska, J. Chandra, and J.E. Flaherty, Eds., "Adaptive Computational Methods for Partial Differential Equations," SIAM, Philadelphia, 1983.
3. I. Babuska, O.C. Zienkiewicz, J.R. Gago, and E.R. de A. Olivera, Eds., "Accuracy Estimates and Adaptive Refinements in Finite Element Computations," John Wiley and Sons, Chichester, 1986.
4. M. Berger and J. Oliger, "Adaptive Mesh Refinement for Hyperbolic Partial Differential Equations," *J. Comput. Phys.*, 53 (1984), 484-512.

5. M. Bieterman, J.E. Flaherty, and P.K. Moore, "Adaptive Refinement Methods for Non-Linear Parabolic Partial Differential Equations," Chap. 19 in *Accuracy Estimates and Adaptive Refinements in Finite Element Computations*, I. Babuska, O.C. Zienkiewicz, J.R. Gago, and E.R. de A. Olivera, Eds., John Wiley and Sons, Chichester, 1986.
6. Q.V. Dihn, R. Glowinski, and J. P\'eriaux, "Solving Elliptic Problems by Domain Decomposition Methods with Applications," in *Elliptic Problem Solvers II*, G. Birkhoff and A. Schoenstadt, Eds., Academic Press, Orlando, 1984, pp. 305-426.
7. J.E. Flaherty and P.K. Moore, "A Local Refinement Finite Element Method for Time Dependent Partial Differential Equations," Trans. Second Army Conf. Appl. Math and Comput., ARO Rep. 85-1, U.S. Army Research Office, 1985, pp. 585-595.
8. R. Glowinski and M.F. Wheeler, "Domain Decomposition and Mixed Finite Element Methods for Elliptic Problems," Research Report UH/MD/-8, Department of Mathematics, University of Houston, 1987.
9. P.K. Moore, "A Local Adaptive Refinement Method for Parabolic Partial Differential Equations in One and Two Space Dimensions," Ph.D. Dissertation, Rensselaer Polytechnic Institute, 1987, in preparation.
10. P.K. Moore and J.E. Flaherty, "A Local Refinement Finite Element Method for One-Dimensional Parabolic Systems," 1987, in preparation.
11. G. Starius, "On Composite Mesh Difference Methods for Hyperbolic Differential Equations," *Numerische Math.*, 35 (1980), pp. 241-255.

12. D.M. Young and T.-Z. Mai, "ITPACK 3A User's Guide" (preliminary version), Report CNA-197, Center for Numerical Analysis, The University of Texas, 1984.

TECHNICAL REPORT INTERNAL DISTRIBUTION LIST

	<u>NO. OF COPIES</u>
CHIEF, DEVELOPMENT ENGINEERING BRANCH	
ATTN: SMCAR-CCB-D	1
-DA	1
-DC	1
-DM *	1
-DP	1
-DR	1
-DS (SYSTEMS)	1
CHIEF, ENGINEERING SUPPORT BRANCH	
ATTN: SMCAR-CCB-S	1
-SE	1
CHIEF, RESEARCH BRANCH	
ATTN: SMCAR-CCB-R	2
-R (ELLEN FOGARTY)	1
-RA	1
-RM	1
-RP	1
-RT	1
TECHNICAL LIBRARY	5
ATTN: SMCAR-CCB-TL	
TECHNICAL PUBLICATIONS & EDITING UNIT	2
ATTN: SMCAR-CCB-TL	
DIRECTOR, OPERATIONS DIRECTORATE	1
ATTN: SMCWV-OD	
DIRECTOR, PROCUREMENT DIRECTORATE	1
ATTN: SMCWV-PP	
DIRECTOR, PRODUCT ASSURANCE DIRECTORATE	1
ATTN: SMCWV-QA	

NOTE: PLEASE NOTIFY DIRECTOR, BENET LABORATORIES, ATTN: SMCAR-CCB-TL, OF ANY ADDRESS CHANGES.

TECHNICAL REPORT EXTERNAL DISTRIBUTION LIST

	<u>NO. OF COPIES</u>		<u>NO. OF COPIES</u>
ASST SEC OF THE ARMY RESEARCH AND DEVELOPMENT ATTN: DEPT FOR SCI AND TECH THE PENTAGON WASHINGTON, D.C. 20310-0103	1	COMMANDER ROCK ISLAND ARSENAL ATTN: SMCRI-ENM ROCK ISLAND, IL 61299-5000	1
ADMINISTRATOR DEFENSE TECHNICAL INFO CENTER ATTN: DTIC-FDAC CAMERON STATION ALEXANDRIA, VA 22304-6145	12	DIRECTOR US ARMY INDUSTRIAL BASE ENGR ACTV ATTN: AMXIB-P ROCK ISLAND, IL 61299-7260	1
COMMANDER US ARMY ARDEC ATTN: SMCAR-AEE SMCAR-AES, BLDG. 321 SMCAR-AET-0, BLDG. 351N SMCAR-CC SMCAR-CCP-A SMCAR-FSA SMCAR-FSM-E SMCAR-FSS-D, BLDG. 94 SMCAR-MSI (STINFO) PICATINNY ARSENAL, NJ 07806-5000	1 1 1 1 1 1 1 1 2	COMMANDER US ARMY TANK-AUTMV R&D COMMAND ATTN: AMSTA-DDL (TECH LIB) WARREN, MI 48397-5000	1
DIRECTOR US ARMY BALLISTIC RESEARCH LABORATORY ATTN: SLCBR-DD-T, BLDG. 305 ABERDEEN PROVING GROUND, MD 21005-5066	1	COMMANDER US MILITARY ACADEMY ATTN: DEPARTMENT OF MECHANICS WEST POINT, NY 10996-1792	1
DIRECTOR US ARMY MATERIEL SYSTEMS ANALYSIS ACTV ATTN: AMXSY-MP ABERDEEN PROVING GROUND, MD 21005-5071	1	US ARMY MISSILE COMMAND REDSTONE SCIENTIFIC INFO CTR ATTN: DOCUMENTS SECT, BLDG. 4484 REDSTONE ARSENAL, AL 35898-5241	2
COMMANDER HQ, AMCCOM ATTN: AMSMC-IMP-L ROCK ISLAND, IL 61299-6000	1	COMMANDER US ARMY FGN SCIENCE AND TECH CTR ATTN: DRXST-SD 220 7TH STREET, N.E. CHARLOTTESVILLE, VA 22901	1
		COMMANDER US ARMY LABCOM MATERIALS TECHNOLOGY LAB ATTN: SLCMT-IML (TECH LIB) WATERTOWN, MA 02172-0001	2

NOTE: PLEASE NOTIFY COMMANDER, ARMAMENT RESEARCH, DEVELOPMENT, AND ENGINEERING CENTER, US ARMY AMCCOM, ATTN: BENET LABORATORIES, SMCAR-CCB-TL, WATERVLIET, NY 12189-4050, OF ANY ADDRESS CHANGES.

TECHNICAL REPORT EXTERNAL DISTRIBUTION LIST (CONT'D)

	<u>NO. OF COPIES</u>		<u>NO. OF COPIES</u>
COMMANDER US ARMY LABCOM, ISA ATTN: SLCIS-IM-TL 2800 POWDER MILL ROAD ADELPHI, MD 20783-1145	1	COMMANDER AIR FORCE ARMAMENT LABORATORY ATTN: AFATL/MN EGLIN AFB, FL 32542-5434	1
COMMANDER US ARMY RESEARCH OFFICE ATTN: CHIEF, IPO P.O. BOX 12211 RESEARCH TRIANGLE PARK, NC 27709-2211	1	COMMANDER AIR FORCE ARMAMENT LABORATORY ATTN: AFATL/MNF EGLIN AFB, FL 32542-5434	1
DIRECTOR US NAVAL RESEARCH LAB ATTN: MATERIALS SCI & TECH DIVISION CODE 26-27 (DOC LIB) WASHINGTON, D.C. 20375	1	METALS AND CERAMICS INFO CTR BATTELLE COLUMBUS DIVISION 505 KING AVENUE COLUMBUS, OH 43201-2693	1

NOTE: PLEASE NOTIFY COMMANDER, ARMAMENT RESEARCH, DEVELOPMENT, AND ENGINEERING CENTER, US ARMY AMCCOM, ATTN: BENET LABORATORIES, SMCAR-CCB-TL, WATERVLIET, NY 12189-4050, OF ANY ADDRESS CHANGES.

END

DATE

FILMED

7-88

Dtic